

University of New Orleans  
**ScholarWorks@UNO**

---

Physics Faculty Publications

Department of Physics

---

2009

## Structural, magnetic, and electronic transport properties of (Sr<sub>0.9</sub>Ca<sub>0.1</sub>)<sub>3</sub>Ru<sub>2</sub>O<sub>7</sub> single crystal

Bin Qian

Zhe Qu

Jin Peng

Tijang Liu

Xiaoshan Wu

*See next page for additional authors*

Follow this and additional works at: [https://scholarworks.uno.edu/phys\\_facpubs](https://scholarworks.uno.edu/phys_facpubs)

 Part of the [Physics Commons](#)

---

### Recommended Citation

J. Appl. Phys. 105, 07E323 (2009)

This Article is brought to you for free and open access by the Department of Physics at ScholarWorks@UNO. It has been accepted for inclusion in Physics Faculty Publications by an authorized administrator of ScholarWorks@UNO. For more information, please contact [scholarworks@uno.edu](mailto:scholarworks@uno.edu).

---

**Authors**

Bin Qian, Zhe Qu, Jin Peng, Tijang Liu, Xiaoshan Wu, L Spinu, and Z Q. Mao

## Structural, magnetic, and electronic transport properties of $(\text{Sr}_{0.9}\text{Ca}_{0.1})_3\text{Ru}_2\text{O}_7$ single crystal

Bin Qian,<sup>1,2,3</sup> Zhe Qu,<sup>1</sup> Jin Peng,<sup>1</sup> Tijiang Liu,<sup>1</sup> Xiaoshan Wu,<sup>2,a)</sup> L. Spinu,<sup>4</sup> and Z. Q. Mao<sup>1</sup>

<sup>1</sup>Physics Department, Tulane University, New Orleans, Louisiana 70118, USA

<sup>2</sup>Department of Physics, Laboratory of Solid State Microstructures, Nanjing University, Nanjing 210093, China

<sup>3</sup>Department of Physics and Jiangsu Laboratory of Advanced Functional Material, Changshu Institute of Technology, Changshu 215500, China

<sup>4</sup>Physics Department and Advanced Material Research Institute, University of New Orleans, New Orleans, Louisiana 70148, USA

(Presented 13 November 2008; received 25 September 2008; accepted 11 December 2008; published online 19 March 2009)

We have studied the structural, magnetic, and electronic transport properties of  $(\text{Sr}_{0.9}\text{Ca}_{0.1})_3\text{Ru}_2\text{O}_7$  using single crystals grown by a floating-zone technique. The structure analysis by Rietveld refinements reveals that the Ca substitution for Sr intensifies the structure distortion; the rotation angle of the  $\text{RuO}_6$  octahedron increases. This structure change tunes magnetic and transport properties dramatically. The magnetic ground state switches from an itinerant metamagnetic state for  $\text{Sr}_3\text{Ru}_2\text{O}_7$  to a nearly ferromagnetic state for  $(\text{Sr}_{0.9}\text{Ca}_{0.1})_3\text{Ru}_2\text{O}_7$ . The Fermi liquid behavior occurs in  $\text{Sr}_3\text{Ru}_2\text{O}_7$ , but is suppressed in  $(\text{Sr}_{0.9}\text{Ca}_{0.1})_3\text{Ru}_2\text{O}_7$ . These results strongly suggest that lattice, spin, and charge degrees of freedom are strongly coupled in this system. The band width narrowing caused by the structure distortion should be responsible for the enhancement of ferromagnetic correlations and the change of transport properties. © 2009 American Institute of Physics. [DOI: 10.1063/1.3074784]

The Ruddlesden–Popper type ruthenates  $(\text{Sr},\text{Ca})_{n+1}\text{Ru}_n\text{O}_{3n+1}$  have been the subject of broad interest in the community of strongly correlated electron system due to a rich variety of novel magnetic and electronic ground state properties such as spin triplet superconductivity,<sup>1</sup> itinerant magnetism,<sup>2</sup> and antiferromagnetic Mott insulator.<sup>3</sup> The double-layered  $(\text{Sr}_{1-x}\text{Ca}_x)_3\text{Ru}_2\text{O}_7$  ( $n=2$ ) system exhibits a complex magnetic phase diagram.<sup>4</sup> The magnetic ground state evolves from an itinerant metamagnet for  $x < 0.08$  to a heavy-mass nearly ferromagnetic state with an extremely large Wilson ratio for  $0.08 < x < 0.4$ . This nearly ferromagnetism (FM) state does not evolve into a long-range FM order despite considerably strong FM fluctuations, but freezes into a cluster spin glass (CSG). When the Ca content is further increased to the  $0.4 < x \leq 1.0$  range, the system switches to an antiferromagnetic state. In addition, non-Fermi liquid behavior occurs as the frozen temperature  $T_{\text{SG}}$  is suppressed to zero near  $x \sim 0.08$ , suggesting the presence of quantum critical behavior near this critical composition.

In this paper, we report detailed studies of structural, magnetic, and electronic transport properties of the sample  $(\text{Sr}_{0.9}\text{Ca}_{0.1})_3\text{Ru}_2\text{O}_7$ , which is close to the critical composition with  $x \sim 0.08$ . Our objective is to further identify the novel quantum phenomena near this critical composition and investigate its underlying physics.

Our sample  $(\text{Sr}_{0.9}\text{Ca}_{0.1})_3\text{Ru}_2\text{O}_7$  was grown using a floating-zone technique and carefully screened by x-ray diffraction and superconducting quantum interference device

(SQUID) magnetometer. Since SQUID has an extremely high sensitivity to ferromagnetic materials, it guarantees that the selected samples do not involve any FM impurity phases such as  $(\text{Sr},\text{Ca})_4\text{Ru}_3\text{O}_{10}$ .<sup>5</sup> Our structure analysis was carried out using general structure analysis system (GSAS) for Rietveld refinement of x-ray diffraction spectra.<sup>6</sup> The x-ray diffraction spectrum was taken in the Bragg–Brentano geometry using powdered single crystals and a step-scan mode with the counting time of 8 s/point. The step-scan size is  $0.02^\circ$ . The measurement was conducted at room temperature. The resistivity measurement was performed using a standard four-probe method.

Figure 1 shows the x-ray diffraction pattern in the range from  $20^\circ$  to  $100^\circ$  for the sample  $(\text{Sr}_{0.9}\text{Ca}_{0.1})_3\text{Ru}_2\text{O}_7$ . The calculated reflection profile shown in Fig. 1 is from the GSAS refinement. No absorption is taken into account during refinements. While the sample has a slightly preferential orientation along the  $c$  axis, good assignments of  $(hkl)$  indices to all the peaks were obtained. The refinement factors are  $R_{\text{wp}} = 5.86\%$ ,  $R_p = 4.33\%$ , and  $\chi^2 = 5.683$ , respectively. Structure parameters derived from the refinement is shown in Table I. We find that the Ca substitution for Sr enhances the structure distortion while the structure of  $(\text{Sr}_{0.9}\text{Ca}_{0.1})_3\text{Ru}_2\text{O}_7$  can still be described with the same space group as that of  $\text{Sr}_3\text{Ru}_2\text{O}_7$ , i.e.,  $Bbcb$  (No. 68). The rotation angle of  $\text{RuO}_6$  octahedron increases from  $6.8^\circ$  for  $\text{Sr}_3\text{Ru}_2\text{O}_7$  to  $9.77^\circ$  for  $(\text{Sr}_{0.9}\text{Ca}_{0.1})_3\text{Ru}_2\text{O}_7$ ; the octahedron rotation is schematically shown in the inset of Fig. 1. This rotation angle slightly increases the orthorhombicity of the unit cell. Such a structure change driven by the octahedron rotation is similar to

<sup>a)</sup>Electronic mail: xswu@nju.edu.cn.

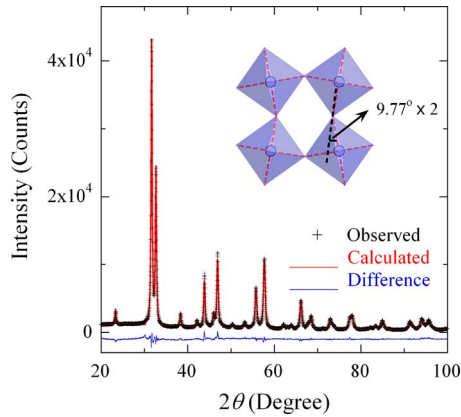


FIG. 1. (Color online) Observed (open circles), calculated (solid line), and different (bottom of the figure) intensities of powder diffraction pattern of the  $(\text{Sr}_{0.9}\text{Ca}_{0.1})_3\text{Ru}_2\text{O}_7$  sample at room temperature.  $R_{\text{wp}}=5.86\%$ ,  $R_p=4.33\%$ , and  $\chi^2=5.683$ . The inset shows the schematic of the octahedron rotation of  $\text{RuO}_6$ .

what is observed in  $\text{Ca}_{2-x}\text{Sr}_x\text{RuO}_4$  when  $0.5 < x < 1.5$ .<sup>7</sup>

The main panel of Fig. 2 shows magnetic susceptibilities  $\chi_{\text{dc}}$  measured at 0.3 T for the samples  $(\text{Sr}_{0.9}\text{Ca}_{0.1})_3\text{Ru}_2\text{O}_7$  and  $\text{Sr}_3\text{Ru}_2\text{O}_7$ . For  $\text{Sr}_3\text{Ru}_2\text{O}_7$ , the susceptibility shows a peak near 15 K; a metamagnetic transition occurs below this peak temperature; the metamagnetic transition field is about 5.5 T at 2 K for  $H\parallel ab$  (see the inset of Fig. 2). All these features are consistent with the results reported previously.<sup>9</sup> In comparison with  $\text{Sr}_3\text{Ru}_2\text{O}_7$ , the susceptibility of  $(\text{Sr}_{0.9}\text{Ca}_{0.1})_3\text{Ru}_2\text{O}_7$  is significantly enhanced and it tends to diverge at low temperatures, suggesting that magnetic correlations are strongly enhanced. The measurement of magnetization as a function of magnetic field  $M(H)$  shows that the metamagnetic transition is suppressed in this sample. The concave characteristic of  $M(H)$  shown in the inset of Fig. 2 indicates that magnetic correlations in this sample should be ferromagnetic. The reversible behavior in  $M(H)$  upon upward and downward field sweeps shows that no long-range ferromagnetic order occurs even at 2 K. In addition, we performed the magnetic susceptibility measurement at a low field, 5 mT for this sample. As shown in Fig. 2(b), we observed an unusual irreversible behavior below 10 K between zero-field-cooling (ZFC) and field-cooling (FC) histories. This irreversible behavior does not seem associated with a spin glassy state since we did not observe any frequency dependence in the ac magnetic susceptibility  $\chi_{\text{ac}}$  of this sample [see the inset of Fig. 2(b)].

Another important feature in  $\chi_{\text{dc}}$  for the sample  $(\text{Sr}_{0.9}\text{Ca}_{0.1})_3\text{Ru}_2\text{O}_7$  is that it follows Curie-Weiss (CW) temperature dependence and the Weiss temperature  $T_{\text{CW}}$  derived from the CW fitting is  $\sim -11$  K, which is in contrast with

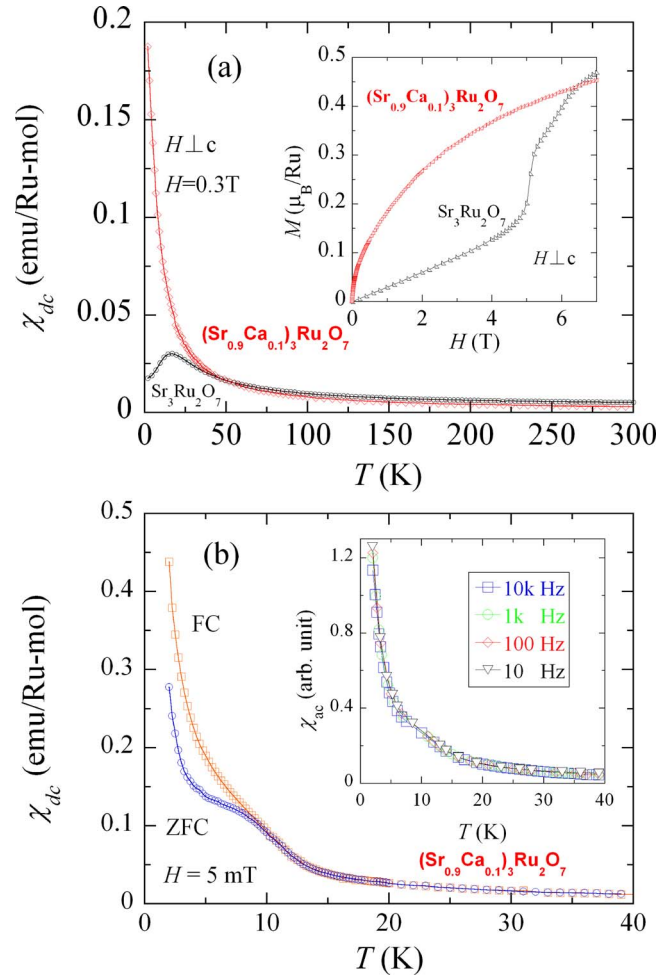


FIG. 2. (Color online) (a) dc magnetic susceptibility measured at 0.3 T for  $\text{Sr}_3\text{Ru}_2\text{O}_7$  and  $(\text{Sr}_{0.9}\text{Ca}_{0.1})_3\text{Ru}_2\text{O}_7$ . (Inset) The magnetization as a function of field at 2 K. (b) dc magnetic susceptibility measured at 5 mT for  $(\text{Sr}_{0.9}\text{Ca}_{0.1})_3\text{Ru}_2\text{O}_7$ . (Inset) The ac magnetic susceptibility measured at various frequencies for  $(\text{Sr}_{0.9}\text{Ca}_{0.1})_3\text{Ru}_2\text{O}_7$ .

$T_{\text{CW}} \sim -40$  K of  $\text{Sr}_3\text{Ru}_2\text{O}_7$ .<sup>10</sup> Previous studies have shown that there exist competing magnetic correlations in  $\text{Sr}_3\text{Ru}_2\text{O}_7$  due to a multiple band effect; both FM and AFM correlations coexist.<sup>11–13</sup> The negative Weiss temperature of  $\text{Sr}_3\text{Ru}_2\text{O}_7$  suggests that AFM correlations dominate its magnetic ground state; this point of view has been confirmed in neutron scattering and nuclear magnetic resonance measurements.<sup>11,12</sup> The decrease in negative Weiss temperature for  $(\text{Sr}_{0.9}\text{Ca}_{0.1})_3\text{Ru}_2\text{O}_7$  suggests that the Ca substitution for Sr suppresses the AFM correlations. The divergent behavior of  $\chi_{\text{dc}}$  at low temperature, as well as the concave characteristic in  $M(H)$  shown in Fig. 2, suggests that FM correlations in  $(\text{Sr}_{0.9}\text{Ca}_{0.1})_3\text{Ru}_2\text{O}_7$  becomes dominant. Our

TABLE I. Results of Rietveld analyses for  $(\text{Sr}_{0.9}\text{Ca}_{0.1})_3\text{Ru}_2\text{O}_7$  using GSAS program. Like in  $\text{Sr}_3\text{Ru}_2\text{O}_7$ , the structure model with the  $Bbcb$  (No. 68) space group yields the best fit for  $(\text{Sr}_{0.9}\text{Ca}_{0.1})_3\text{Ru}_2\text{O}_7$ . For comparison, the structure parameters of  $\text{Sr}_3\text{Ru}_2\text{O}_7$  (taken from Ref. 8) are also included in the table.

	$a$ (Å)	$b$ (Å)	$c$ (Å)	Rotation angle (deg)	Tilting angle (deg)
$\text{Sr}_3\text{Ru}_2\text{O}_7$	5.5006(4)	5.5006(4)	20.7250(1)	6.80	0
$(\text{Sr}_{0.9}\text{Ca}_{0.1})_3\text{Ru}_2\text{O}_7$	5.4827(2)	5.4916(2)	20.6998(5)	9.77	0

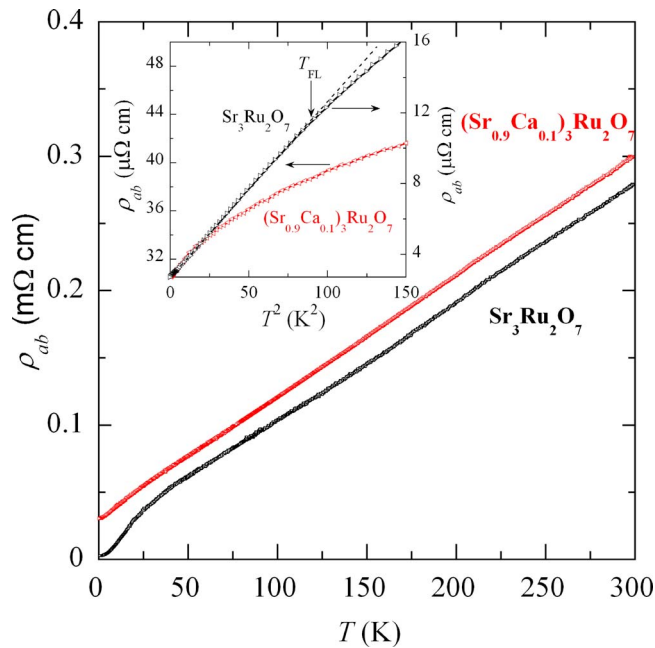


FIG. 3. (Color online) In-plane resistivity as a function of temperature for  $(\text{Sr}_{0.9}\text{Ca}_{0.1})_3\text{Ru}_2\text{O}_7$  and  $\text{Sr}_3\text{Ru}_2\text{O}_7$ . (Inset)  $\rho_{ab}$  vs  $T^2$  at low temperatures.

preliminary neutron scattering measurements on this sample provides a strong support for this point of view.<sup>14</sup>

This evolution of magnetic ground state from  $\text{Sr}_3\text{Ru}_2\text{O}_7$  to  $(\text{Sr}_{0.9}\text{Ca}_{0.1})_3\text{Ru}_2\text{O}_7$  can be well understood in terms of the structure change caused by the Ca substitution for Sr. As discussed above, the Ca substitution for Sr results in the increase in rotation angle of  $\text{RuO}_6$  octahedron. According to the first-principles calculation for  $\text{Ca}_{2-x}\text{Sr}_x\text{RuO}_4$ ,<sup>15</sup> such an increase in octahedron rotation angle would narrow band width, which thus increases the density of state (DOS) near the Fermi surface. On the basis of Stoner theory, the increase in DOS near the Fermi level should drive the system toward a FM instability, which is consistent with our observations. On the other hand, the octahedron rotation reduces the symmetry to some extent and therefore changes the shape of Fermi surface. As a result, the Fermi surface nesting, which is responsible for the AFM correlation, is weakened. Regarding the irreversibility of  $\chi_{dc}$  between ZFC and FC at low fields, we have not understood its origin. This certainly deserves further investigation.

As shown in Fig. 3, electronic transport properties exhibit a dramatic change with the variation in magnetic ground state for  $(\text{Sr}_{0.9}\text{Ca}_{0.1})_3\text{Ru}_2\text{O}_7$ . In  $\text{Sr}_3\text{Ru}_2\text{O}_7$ , the in-plane resistivity  $\rho_{ab}$  shows a downturn below 15 K, which is the characteristic temperature for the metamagnetic transition, while in  $(\text{Sr}_{0.9}\text{Ca}_{0.1})_3\text{Ru}_2\text{O}_7$ , this downturn feature is suppressed. The inset of Fig. 3 shows their resistivities at low temperatures on the  $T^2$  scale.  $\text{Sr}_3\text{Ru}_2\text{O}_7$  exhibits a typical Fermi liquid behavior, i.e.,  $\rho_{ab}(T) \propto T^2$ ; the Fermi liquid temperature  $T_{FL}$  is about  $\sim 10$  K. For  $(\text{Sr}_{0.9}\text{Ca}_{0.1})_3\text{Ru}_2\text{O}_7$ , however, the Fermi liquid behavior is completely suppressed and

its  $\rho_{ab}(T)$  can be fitted with a powerlaw temperature dependence  $T^n$  ( $n \sim 2.3$ ) for  $T < 2$  K. This powerlaw behavior is likely associated with the spin scattering since the nearly FM state of this sample is possibly frozen into the CSG phase at temperatures below 2 K.

In summary, we have investigated structural, magnetic, and electronic transport properties of double-layered  $(\text{Sr}_{0.9}\text{Ca}_{0.1})_3\text{Ru}_2\text{O}_7$  solid solution. We found that from  $\text{Sr}_3\text{Ru}_2\text{O}_7$  to  $(\text{Sr}_{0.9}\text{Ca}_{0.1})_3\text{Ru}_2\text{O}_7$  the magnetic ground state switches from a metamagnetic state to a nearly FM state. In this nearly FM state, an unusual irreversible behavior between ZFC and FC in magnetic susceptibility at low fields was observed and the Fermi liquid behavior seen in  $\text{Sr}_3\text{Ru}_2\text{O}_7$  was suppressed. Such changes in magnetic and electronic properties can be attributed to the increase in the rotation angle of  $\text{RuO}_6$  octahedron caused by the Ca substitution for Sr. These observations suggest that lattice, spin, and charge degrees of freedom in double-layered ruthenates are strongly coupled.

The work at Tulane is supported by the NSF under Grant No. DMR-0645305, the DOE under Grant No. DE-FG02-07ER46358, and the Research Corporation. Work at UNO is supported by DARPA through Grant No. HR0011-07-1-0031. Work at Nanjing University is supported by NNSFC (Grant Nos. 10474031 and 10523001). X.W. would like to thank the State Key Project of Fundamental Research Contract Nos. 2006CB921802 and NCET-04-0463. B.Q. likes to give his thanks to the NSF of Jiangsu Education Department Grant No. 07KJD140001.

- <sup>1</sup>A. P. Mackenzie and Y. Maeno, *Rev. Mod. Phys.* **75**, 657 (2003).
- <sup>2</sup>P. B. Allen, H. Berger, O. Chauvet, L. Forro, T. Jarlborg, A. Junod, B. Revaz, and G. Santi, *Phys. Rev. B* **53**, 4393 (1996).
- <sup>3</sup>S. Nakatsuji and Y. Maeno, *Phys. Rev. Lett.* **84**, 2666 (2000).
- <sup>4</sup>Z. Qu, L. Spinu, H. Q. Yuan, V. Dobrosavljevic, W. Bao, J. W. Lynn, M. Nicklas, J. Peng, T. J. Liu, D. Fobes, E. Flesch, and Z. Q. Mao, *Phys. Rev. B* **78**, 180407(R) (2008).
- <sup>5</sup>S. Chikara, V. Durairaj, W. H. Song, Y. P. Sun, X. N. Lin, A. Douglass, G. Cao, P. Schlottmann, and S. Parkin, *Phys. Rev. B* **73**, 224420 (2006).
- <sup>6</sup>A. C. Larson and R. B. Von Dreele, Los Alamos National Laboratory Report LAUR **86**, 748 (1985).
- <sup>7</sup>O. Friedt, M. Braden, G. Andre, P. Adelman, S. Nakatsuji, and Y. Maeno, *Phys. Rev. B* **63**, 174432 (2001).
- <sup>8</sup>H. Shaked, J. D. Jorgensen, O. Chmaissem, S. Ikeda, and Y. Maeno, *J. Solid State Chem.* **154**, 361 (2000).
- <sup>9</sup>R. S. Perry, L. M. Galvin, S. A. Grigera, L. Capogna, A. J. Schofield, A. P. Mackenzie, M. Chiao, S. R. Julian, S. I. Ikeda, S. Nakatsuji, Y. Maeno, and C. Pfleiderer, *Phys. Rev. Lett.* **86**, 2661 (2001).
- <sup>10</sup>S. Ikeda, Y. Maeno, and T. Fujita, *Phys. Rev. B* **57**, 978 (1998).
- <sup>11</sup>L. Capogna, E. M. Forgan, S. M. Hayden, A. Wildes, J. A. Duffy, A. P. Mackenzie, R. S. Perry, S. Ikeda, Y. Maeno, and S. P. Brown, *Phys. Rev. B* **67**, 012504 (2003).
- <sup>12</sup>K. Kitagawa, K. Ishida, R. S. Perry, T. Tayama, T. Sakakibara, and Y. Maeno, *Phys. Rev. Lett.* **95**, 127001 (2005).
- <sup>13</sup>J. Hooper, M. H. Fang, M. Zhou, D. Fobes, N. Dang, Z. Q. Mao, C. M. Feng, Z. A. Xu, M. H. Yu, C. J. O'Connor, G. J. Xu, N. Anderson, and M. Salamon, *Phys. Rev. B* **75**, 060403 (2007).
- <sup>14</sup>W. Bao, Z. Q. Mao, Z. Qu, and J. W. Lynn, *Phys. Rev. Lett.* **100**, 247203 (2008).
- <sup>15</sup>Z. Fang and K. Terakura, *Phys. Rev. B* **64**, 020509 (2001).